Ecological Factors and Jaw Morphology in Lepidosauria: A Geometric Morphometric and Biomechanical Approach

Ecological Factors and Jaw Morphology in Lepidosauria: A Geometric Morphometric and Biomechanical Approach

Robert Noble

A Thesis in the Field of Biology

for the Degree of Master of Liberal Arts in Extension Studies

Harvard University

May 2023

Abstract

Lepidosauria consists of two reptilian orders, with squamates, the larger of the orders, consisting of about 11,000 species that are widespread globally. As a group, lepidosaurs are very diverse in habitat, leg development, dietary behavior, and overall morphology. This study aims to reveal whether ecological inferences can be made on extant squamate taxa based on their jaw morphology as was the case for mammal jaws and squamate skulls and to determine if we can test the rate of change in mandible shape over time. To achieve these objectives, this study employs landmark-based geometric morphometrics and evaluation of biomechanical markers to elucidate relationships between squamate jaw morphology and ecological niches. This study establishes connections between limb development and anterior mechanical advantage, posterior mechanical advantage, and overall jaw shape. Connections between jaw shape evolution and limb development and habitat are also noted here. Further, anterior mechanical advantage can distinguish carnivorous and omnivorous taxa as well as fossorial and terrestrial taxa.

Frontispiece

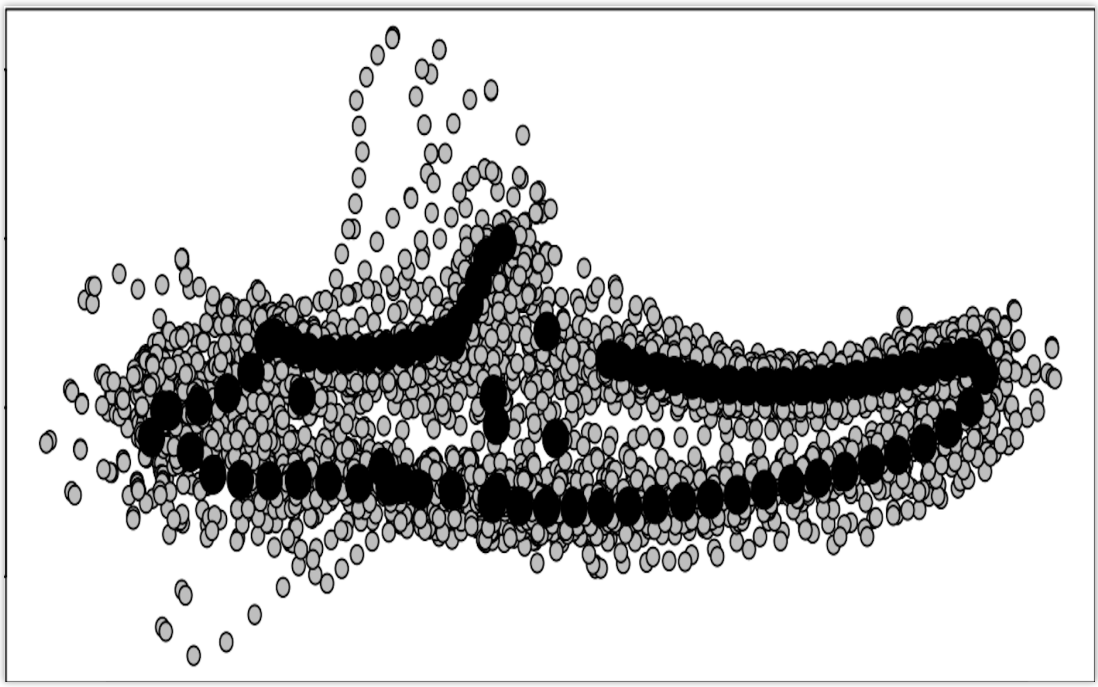

Acknowledgments

I'd like to thank Dr. Stephanie Pierce for allowing me to join the lab to complete this thesis project.

I am appreciative of the opportunity. I would like to offer special thanks to Dr. Tiago Simões for your continued hands-on supervision, mentorship, and pointing me to the appropriate resources to be successful in this project. I value all the guidance and wealth of knowledge you have provided.

I would also like to thank Jim Morris, my research advisor for helping me navigate the thesis process, being amenable to my questions from an administrative standpoint.

Table of Contents

List of Tables

List of Figures

Chapter I:

Introduction

Taxonomy of Squamates and Rhynchocephalians

Lepidosauria consists of two reptilian orders, Squamates and Rhynchocephalians (Figure 1). Squamates, the larger of the orders, consist of about 11,000 species and are widespread globally (except in Antarctica). Dating back to at least 242 million years ago, this group consists of lizards, snakes, and amphisbaenians (Simões & Pyron, 2021).

Sphenodon, the only extant genus of rhynchocephalian, exclusively inhabits islands of New Zealand and shares a common ancestor with squamates that lived ca. 260 Mya (Simões & Pyron, 2021). This genus, having been described as a "living fossil", was originally misclassified as a primitive lizard (Herrera-Flores, Stubbs, Benton, & Ruta, 2017). One key feature in *Sphenodon* that led to this notion was the presence of a cranial lower temporal bar (a feature that is absent in all extant squamates). However, fossil evidence demonstrates the lower temporal bar was already absent in the most recent common ancestors to squamates and rhynchocephalians; therefore, *Sphenodon* must have reacquired the lower temporal bar as an adaptation (Evans & Jones, 2010). *Sphenodon* is almost entirely insectivorous or carnivorous, though some individuals may feed on plant matter (Schwenk, 2000). In contrast, Mesozoic rhynchocephalians had diverse feeding ecologies, encompassing insectivores, opportunistic carnivores, venomous predators, and specialized herbivores (Evans & Jones, 2010).

Estimates based on molecular and morphological clocks suggest squamates and rhynchocephalians first appeared in the Late Permian (Simões & Pyron, 2021). Paramacellodidae, Borioteiiodea/Polyglyhanodontidae, and Mosasauria are all important fossil groups of squamates (Simões & Pyron, 2021). Paramacellodidae, characterized by their rectangular osteoderms, were a group of seemingly terrestrial lizards from the Jurassic (Alifanov, 2019) to Late Cretaceous (Bittencourt, Simoes, Caldwell, & Langer, 2020). Though they are still relatively poorly known in terms of taxonomic and morphological diversity due to their patchy fossil record, this group is the oldest squamate clade to achieve multicontinental occupancy and diversification (Bittencourt et al., 2020). In addition to rectangular osteoderms, this group is also characterized by labiolingually expanded teeth, a rare occurrence in squamates. In contrast, Borioteiiodea, a group from the Late Cretaceous, had some of its members evolving molar-like multicuspid dentition similar to that of mammals (Simões & Pyron, 2021). Interestingly, like *Sphenodon*, two borioteiiod species also possessed a complete lower temporal bar (Simões & Caldwell, 2021). Mosasauria is a group of aquatic, extinct squamates from about 98 Mya to about 66 Mya (Polcyn, Jacobs, Araújo, Schulp, & Mateus, 2014). Members of this group were present on every continent, including Antarctica (Polcyn et al., 2014).

One of the most conspicuous and diverse groups of squamates with extant representatives is Serpentes (snakes) with 3900 species. Members of this group are characterized by their elongate and limb-reduced bodies (Simões & Pyron, 2021). They occupy fossorial, arboreal, terrestrial, and aquatic environments, and live in climates ranging from arid deserts to the open ocean (Hsiang et al., 2015). Many species have

specialized recurved dentition that allows for swallowing of large prey (Simões & Caldwell, 2021). Though dietary niches differ among species, there are no herbivorous species of snake. In fact, most species have evolved specialized jaw-based prehension to aid in capturing animal prey (Schwenk, 2000). Almost all snakes swallow their prey whole, though there are few exceptions, as is the case with termite decapitation in *Indotyphlops braminus* (Mizuno & Kojima, 2015).

The main taxonomic groups of snakes are Scolecophidia, Henophidia, and Caenophidia. Scolecophidia, the blind snakes and thread snakes, includes the Families Anomalepididae, Typhlopidae, Leptotyphlopidae, Gerrhopilidae, and Xenotyphlopidae (Uetz, 2021) and feed on small invertebrate prey (Rieppel, 1979). Henophidia includes pythons, boas, pipe snakes, sunbeam snakes, and shield tails (Simões & Pyron, 2021). Caenophidia, the advanced snakes, are the most common group of snakes worldwide and include colubrids, viperids, diapsids, and elapids (Simões & Pyron, 2021). Scolecophidia are considered to be the earliest diverging group of extant snakes based on molecular data.

Anguimorpha, consisting of ~250 species (Simões & Pyron, 2021), is a diverse clade of lizards (Conrad, Ast, Montanari, & Norell, 2011). One group within Anguimorpha is Varanidae, which includes monitor lizards such as the *Varanus salvator* and the Komodo dragon (*Varanus komodoensis*), the largest non-ophidian squamate in the world today. Varanids have the largest variation in size among all lizards, varying in mass from 8 grams to 100 kilograms. Komodo dragons can grow up to 3 meters long (and run up to 20 kilometers per hour), allowing them to hunt relatively large prey such as deer and boar. In addition to size and speed, serrate teeth, sharp claws, and saliva with

anticoagulant and shock-inducing properties allow for hunting such large prey (Lind et al., 2019). Other groups of Anguimorphs include Helodermatidae, partially comprised of beaded lizards and the Gila monster (*Heloderma suspectum*); Xenosauridae (e.g. the Mexican knob scaled lizards); Shinisauridae (e.g. the Chinese crocodile lizard); Anniellidae (American legless lizards); Diploglossidae (galliwasps); and Anguidae, comprised of alligator lizards, glass lizards, and slow worms (Simões & Pyron, 2021).

Scinoidea are a clade of squamates characterized by hard shiny dorsal scales or forms of plate armor and include Scinidae (skinks), Gerrhosauridae (plated lizards), Cordylidae (girdled lizards), and Xantusiidae (night lizards) (Simões & Pyron, 2021).

Lacertoidea consists of ~1000 species of squamates and are classified into Lacertidae (wall or true lizards), Gymnophthalmidae (spectacled lizards), and teiids (Simões & Pyron, 2021).

Gekkota, containing around 2000 species, have reduced, irregular granular scales and expanded toe pads to allow many species to scale vertical surfaces, even upside down using Van der Waals interactions (Simões & Pyron, 2021). This feature may have independently evolved several times in gekkotan species (Gamble, Greenbaum, Jackman, Russell, & Bauer, 2017).

Dibamidae, consisting of around 25 species, are the insectivorous “blind skinks”, with limbless or limb-reduced bodies and represent one of the earliest modern groups of squamates to evolve, along with gekkotans (Simões & Pyron, 2021). Typically, females are limbless, while males are limb-reduced, having small flaps (Greer, 1985).

Iguania is a clade of squamates that consists of ca. 2000 species, characterized by lobular, fleshy tongues, and include insectivorous anoles, and is subdivided into two main

groups, Acrodonta, and Pleurodonta, with Pleurodonta inhabiting Neotropical regions of the Americas and Acrodonta occupying Old World continents (Simões & Pyron, 2021). Acrodonta includes chameleons and agamas. Interestingly, chameleons have a defining set of morphological characteristics that set them apart from all other lizards, including gripping feet, independently moving eyes, a ballistic tongue, and prehensile tail (R. Andrews, 2015). Most chameleons develop more varied diets as they grow, increasing their range of food sizes as they get larger, so that the largest members include both vertebrate and invertebrate prey in their diet (R. Andrews, 2015). Like other lizards, chameleons also feed on plants to supplement water intake (R. Andrews, 2015). Most pleurodont iguanians have multicuspid teeth that are adapted to cropping vegetation (Simões & Caldwell, 2021).

Head Anatomy

Several bone and muscle groups in the head are important to squamate bite mechanics. The most anterior bone on the skull is the premaxilla, with the maxilla lying posterior to it (De Iuliis & Pulerà, 2011). Together, the maxilla and premaxilla contain the upper row of teeth. While in most squamates the premaxilla and maxilla are sutured to each other, in snakes the premaxilla and maxilla are connected by ligaments only, and additional sets of teeth arise from the palatine and pterygoid (De Iuliis & Pulerà, 2011). Posterior to the maxilla is the jugal, lacrimal, and prefrontal, with the postfrontal lying posterior to the frontal and articulating with the squamosal at its posterior end (De Iuliis & Pulerà, 2011). The postorbital articulates with both the postfrontal and the jugal at their lateral ends. The epipterygoid is a slender, cylindrical bone that articulates ventrally with the pterygoid and dorsally with the parietal, which is posterior to the postfrontal (De

Iuliis & Pulerà, 2011). Ventral to the parietal are all the bones from the braincase (De Iuliis & Pulerà, 2011). Posterior and ventral to these bones lies the quadrate, a large, curved, and posteriorly concave bone that serves as the origination point for many adductor muscles (De Iuliis & Pulerà, 2011; Oelrich, 1956).

The mandibular joint is formed by the articulation of the head of the quadrate with the articular fossa (condyle) of the articular bone on the mandible (Oelrich, 1956). Posterior to the condyle is the retroarticular process (Oelrich, 1956). The jaws are paired rami that are united anteriorly, bear teeth anteriorly on the dentary bone whereas the post-dentary elements provide area of insertion for the jaw adductor muscles (Oelrich, 1956). Each ramus is composed of six separate bones: articular+prearticular (fused together), angular, surangular, splenial, dentary, and coronoid (Oelrich, 1956)(Figure 2). In snakes, however, the surangular also becomes fused to the articular+prearticular to form one compound bone (De Iuliis & Pulerà, 2011).

Anterior and ventral to the articular is the angular. The angular is an elongate flattened bone, the posterior part of which forms the ventral surface of the jaw between the articular and surangular bones. The surangular, which is dorsal to the angular, forms the lateral wall of the posterior third of the mandible and the lateral rim of the mandibular foramen. The anterior process projects into the dentary bone, which articulates anteriorly and contains a row of teeth (Oelrich, 1956). The coronoid has a dorsally extending process, the insertion point for the bodenaponeurosis, a common tendon of insertion of the adductor musculature (De Iuliis & Pulerà, 2011; Oelrich, 1956). The process lies beside other anterior and posterior processes that connect it with the dentary, surangular, splenial, and articular bones. The bodenaponeurosis is not present in most snakes, and

snakes that do possess it show adductor insertion patterns different from lizards with respect to this tendon (Haas, 1973). The splenial articulates with all the other mandibular bones, except the articular+prearticular in some groups (Oelrich, 1956).

The adductor muscles are grouped into three main divisions: the *adductor mandibularis externus*, the *adductor mandibularis internus*, and the *adductor mandibularis posterior.* The *adductor mandibularis externus* can be further segregated into the *superficialis*, the *medius*, and the *profundus* (Haas, 1973; Oelrich, 1956). The *superficialis* part is made up of two relatively distinct muscles, the *levator angularis oris* and the *superficialis* (Oelrich, 1956). The *adductor mandibularis internus* can be separated into two distinct muscle masses: the *pterygomandibularis* and the *pseudotemporalis* (Haas, 1973; Oelrich, 1956).

The *adductor mandibularis externus* is an important muscle group for applying hard bites (Jones, Curtis, O'Higgins, Fagan, & Evans, 2009). The *adductor mandibularis externus superficialis* is the most lateral part of the *adductor mandibularis externus* to insert into the bodenaponeurosis (Oelrich, 1956). It originates from the quadrate, squamosal, and from the inferior, medial, and dorsal borders of the postorbital bone, with its most anterior fibers coming only from the dorsal border of the postorbital (Haas, 1973; Oelrich, 1956). The *levator angularis oris* originates from the quadrate, squamosal, and postorbital bones, extending to the point where the postorbital joins the jugal (Oelrich, 1956).

The *adductor mandibularis externus medius* is medial to the *superficialis*, dorsal to the parietal bone and *M. a. m. e. profundus*, and posterolateral to the *M. a. m. i. pseudotemporalis* (Oelrich, 1956). It originates from the squamosal, the parietal, the

supratemporal, and the quadrate [postorbital and parietal in *Sphenodon* (Haas, 1973)] and inserts at the surangular, the coronoid, and the bodenaponeurosis (Oelrich, 1956). The *M. a. m. e. Profundus* originates from the parietal, supratemporal, and the prootic and bodenaponeurosis (Oelrich, 1956). It is important to note that this muscle is absent in most snakes (McDowell, 1986).

The *M. adductor mandibularis internus* is composed of two muscle masses, the *pseudotemporalis* and the *pterygomandibularis* (Oelrich, 1956), and is an important muscle for closing the mouth as well a jaw protraction (Jones et al., 2009). The *pseudotemporalis* has two parts, *superficialis* and *profundus* (Oelrich, 1956). However, the *profundus* is absent in Gekkota and in snakes (Haas, 1973). The *pseudotemporalis superficialis* originates from the parietal bone, the epipterygoid, and the prootic bone and inserts into coronoid at the bodenaponeurosis (Haas, 1973; Oelrich, 1956). The *profundus* originates from the epipterygoid and inserts into the coronoid and the articular bone (Haas, 1973; Oelrich, 1956). The *pterygomandibularis* is the largest muscle in the head and forms the greater part of the adductor musculature of the jaw, exerting several forces in adducting the jaw and in closing the mouth (Oelrich, 1956). In *Sphenodon*, it is further divided into 2 factions: the *typicus* and *atypicus* (Haas, 1973). It originates from the ectopterygoid and pterygoid and inserts at several points of the articular (Oelrich, 1956).

Research Problem

Studies on jaw shape and biomechanical analyses have revealed correlations between jaw morphology and ecological niche. For example, one study compared the jaws of extant taxa of mammals with known dietary modes (carnivore, insectivore, omnivore, or herbivore) to those of extinct taxa (Morales-García, et al., 2021). Examining

the morphology of their chosen taxa, they were able to elucidate relationships between dietary modes and mechanical advantage of the masseter, mechanical advantage of the temporalis, and overall jaw shape, with similar findings in both extinct and extant taxa of known diets. One broader implication of the results was that jaw morphology could be used as a predictor of dietary mode for extinct species of mammals of unknown diets. Other studies have linked other ecological niches and evolutionary changes of squamates to their skull morphology. For example, two studies demonstrated links between skull size and shape evolution and habitat (Da Silva et al., 2018; Watanabe et al., 2019). Further, Watanabe et al. (2019) noted diet as a having an influence on skull shape.

This study adapts similar geometric morphometric techniques and biomechanical evaluations from the aforementioned studies to the jaws of several taxa of squamates (snakes and lizards) plus *Sphenodon*. Using established datasets along with museum specimens and CT scans, morphometric and biomechanical data were generated and analyzed to identify macroevolutionary patterns and uncover any correlations between form, function, and behavior. Data and specimens will be representative of extant taxa of squamates. One aim of this study was to reveal whether ecological inferences can be made on extant squamate taxa based on their jaw morphology as was the case for mammal jaws and squamate skulls. If the evidence does support this notion, further predictions can be made of environmental landscape of a certain point in geological time when evaluating extinct taxa.

Chapter II:

Materials and Methods

Geometric Morphometrics

Landmark-based geometric morphometrics is a technique used to compare and analyze the shape attributes of two or more objects. In the biological sciences, this approach can be used to compare the evolution of shape among different species, or intraspecifically (e.g. comparative morphology of a species at various developmental stages). It is important to note that shape refers to relative configuration of points on an object, discounting orientation, size, and location of that object (Zelditch, Swiderski, & Sheets, 2012).

The first step in this analysis is to select comparable (i.e., homologous) landmarks on the specimens of interest. These landmarks can be recorded in two or three dimensions (Zelditch et al., 2012). While biological specimens are inherently three-dimensional, two-dimensional landmarking can offer simplified data collection as three-dimensional landmarking can be expensive and time consuming (Zelditch et al., 2012). This is especially true if distances between landmarks in two dimensions is significantly larger than those in the third dimension or if the third dimension is not relevant to a particular analysis (Zelditch et al., 2012).

It is important to select specimens closely related enough such that adequate corresponding landmarks can be identified across specimens (Zelditch et al., 2012). When determining landmarks, four criteria must be met: landmarks must be homologous,

have the same relative orientation across specimens, provide adequate coverage of specimens, be found consistently among specimens, and, for 2D analyses, lie within the same plane (Webster & Sheets, 2010; Zelditch et al., 2012). Once the landmarks have been determined, they must be plotted digitally on photographs of the specimens (so it is important that high quality photographs or CT scans of specimens are obtained).

In addition to homologous landmarks, semi-landmarks can also be used. Semi-landmarks are usually placed connecting homologous landmarks, supplementing shape information, especially when homologous landmarks are sparsely distributed (Webster & Sheets, 2010). Specifically, semi-landmarks can better capture curve shapes between landmarks (Webster & Sheets, 2010; Zelditch et al., 2012). Semi-landmarks on a curve can be determined as increments along curve length or increments of an angle subtended by a curve (Zelditch et al., 2012).

The next step is to use Procrustes superimposition to align landmarks and semi-landmarks (Webster & Sheets, 2010; Zelditch et al., 2012). This procedure transforms all datasets to remove elements of orientation, size, and location (Webster & Sheets, 2010; Zelditch et al., 2012). After these modifications are made, the points can be plotted on a Partial Procrustes diagram, where all landmarks from all sampled specimens are centered around a centroid (Webster & Sheets, 2010). After removal of orientation, size, and location information, and placed under a common coordinate grid, all differences between specimens represent differences in shape only and can be evaluated using multivariate statistical tools.

One of the primary analyses of interest is measuring the amount of shape variation across all specimens (morphological/shape disparity or diversity). Analysis of

shape disparity can be assessed through principal component analysis (PCA), which first identifies patterns of variable covariation by constructing a variance-covariance matrix. The strongly covariate variables are grouped together as principal component axes (PCs), which are then ranked according to how much they explain the total variance in the data. The PCs explaining most of the variance in the data can be used to create two-dimensional plots displaying the distribution of the data on a Cartesian plane — in this case, variation in mandibular shape. Groups of specimens can be created based on specific parameters of interest, such as taxonomic group or feeding ecology (Webster & Sheets, 2010), to detect the total amount of mandibular shape variation within each group. Further, discriminant analyses such as linear discriminant analysis (LDA)— also known as canonical variate analysis (CVA)—can indicate whether we can use shape information to discriminate among groups of interest, and thus, classify species according to a grouping variable (e.g., feeding ecology) based on mandibular shape data (Morales-García, Gill, Janis, & Rayfield, 2021).

This project includes a two-dimensional geometric morphometric analysis for several taxa of squamates and *Sphenodon*. Specimens were acquired from images of museum samples, CT scans from https://www.morphosource.org, and images from digimorph.org. A list of taxa included in this study is given in Table 1. Ecological features evaluated here are dietary mode (carnivore, herbivore, or omnivore), leg development, and habitat. Of note, all faunivorous taxa included in this study are designated as carnivores (see Table 1).

CT images were processed using Dragonfly ORS software (ORS, 2020) to generate two-dimensional images of the lateral jaw. Seventeen landmarks (and curves to

which semi-landmarks were appended) were digitized in TPSDig2 (Rohlf, 2017) and are in are given in Figure 3. Landmarks were digitized on the lateral side of the right mandible for most taxa. For taxa which a right mandible specimen was unavailable, images of the left mandible were mirrored to conserve consistent orientation among specimens. Sliding semi-landmarks were appended to curves in RStudio using package geomorph (Adams, 2022; Baken, 2021). Generalized Procrustes Analysis, principal component analysis, deformation grid generation, and Procrustes ANOVA were also carried out in geomorph (Adams, 2022; Baken, 2021). Deformation grids were used to qualify theoretical morphological disparity along each principal component axis. Linear discriminant analysis was carried out in RStudio using package MASS (Venables, 2002). Comparative rates of jaw shape evolution and phylogenetic signals were calculated using the compare.evol.rates and physignal commands, respectively, in geomorph (Adams, 2022; Baken, 2021).

Biomechanical Analysis

In addition to making geometric morphometric computations, I examined several biomechanical variables, many of which were noted in literature pertaining to biomechanics of archosaur jaws (Stubbs, Pierce, Rayfield, & Anderson, 2013). Though these measurements and markers are simplified versions of reality, they have been shown to be useful in comparative contexts as they relate form to ecological niche (Stubbs et al., 2013):

1) The first metric is total mandibular length, which is the distance between the anterior and posterior ends of the jaw. Mandibular length serves as a proxy for gape size,

which has been shown to have a negative relationship with biting performance (Bourke, Wroe, Moreno, McHenry, & Clausen, 2008).

2) Quadrate/articular offset, which is the perpendicular distance from the mandibular joint to a line running through the bottom row of teeth (Stubbs et al., 2013). This is calculated by superimposing a tangent line on the dorsal surface of the dental row and measuring the orthogonal distance from that line to the point of jaw articulation (Stubbs et al., 2013). Small offset distances are characteristic of the scissor-like jaw opening of carnivores, whereas larger distances are attributed to the viselike-like jaw opening of herbivores (Anderson, 2009; Ramsay & Wilga, 2007).

3) Relative length of dental row is the lengthwise ratio of tooth-bearing bone to total mandibular length. A larger proportion of tooth-bearing bone could indicate more variation in bite force, speed, and overall functional variability. That is, the higher this metric, the larger the range of bite forces due to varied mechanical advantages along the dentition (Anderson, 2009). This measure is the proportion of the length of the jaw that bears teeth relative to total jaw length (Stubbs et al., 2013).

Mechanical advantage is a measure of bite force as a result of the force exerted by the muscle (Gill et al., 2014; Morales-García et al., 2021; Westneat, 2003). Mechanical advantage is calculated by taking the ratio of the length of the inlever to the length of the outlever (Gill et al., 2014; Morales-García et al., 2021; Westneat, 2003). A low mechanical advantage indicates a quick but weak bite, while a high mechanical advantage indicates a strong but slower bite (Morales-García et al., 2021; Wainwright & Richard, 1995). Here, I calculated three classes of mechanical advantage: 4) anterior mechanical advantage, 5) posterior mechanical advantage, and 6) opening mechanical

advantage. For anterior mechanical advantage, the outlever is the distance from the fulcrum (here, the mandibular joint) to anteriormost dental element (Stubbs et al., 2013). The inlever is the distance from the fulcrum to mid-point of adduction musculature insertion. Here, I will select the coronoid as the point of muscular insertion, as it is the insertion point for much of the jaw musculature (Haas, 1973; Oelrich, 1956). Posterior mechanical advantage follows the same principles as anterior mechanical advantage; however, the outlever is the distance from the posteriormost dental point to the fulcrum. For opening mechanical advantage, the outlever is the distance from the fulcrum to the anteriormost tooth, where the inlever is from the fulcrum to the end of the retroarticular process (Stubbs et al., 2013). This metric has been linked to feeding patterns and prey selection (Anderson & Westneat, 2007).

Measurements were taken in ImageJ (Schneider, Rasband, & Eliceiri, 2012) using the same images from the geometric morphometric analysis and are diagramed in Figure 4. Measurements for total mandibular length were standardized by dividing the raw measurements by the calculated centroid sizes from the geometric morphometric analysis. One-way PERMANOVA tests were performed in PAST4 (Hammer, Harper, & Ryan, 2001) for each ecological category and biomechanical measurement combination to evaluate statistically significant differences between groups.

Chapter III:

Results

Geometric Morphometrics

Principal component analysis revealed that PC1 and PC2 accounted for 41.8% and 16.6% of the variation in the data, respectively (Figure 6). Deformation grids generated from the principal component analysis revealed that taxa with low PC1 scores had shorter relative dentaries compared to those with high PC1 scores (Figure 5). Taxa with low PC2 scores have overall longer jaws compared to those with high PC2 scores. Convex hulls indicated a clear separation of amphisbaenians, dibamids, and Sphenodon along both PC1 and PC2 axes. Snakes showed good separation but had some overlap with anguiformes. There was lots of overlap amongst other taxonomic groups.

There was considerable overlap of convex hulls for dietary groups, with carnivores nearly encompassing the other groups. Of note, however, major outliers that contribute to the increase area of the hull were snakes, amphisbaenians, and Sphenodon. There was some separation between limbless and four-legged taxa along the PC1 axis. There was no clustering of taxa by habitat except for semi-fossorial. Similar results were observed in phylogeny-corrected component analysis (Figure 8).

Linear discriminant analysis provides much more separation between groups than does PCA. There is no overlapping of the groups based on diet or for leg development. There is considerable overlap in between groups for habitat, except for fossorial; combination terrestrial and arboreal; semi-fossorial; combination saxicolous and arboreal;

and combination semi-aquatic, arboreal, and terrestrial, with the latter three groups each having only one representative. However, despite any separation along linear discriminants, Procrustes ANOVA determined that differences in leg development and habitat were the only significantly disparate groups based on jaw morphology (Table 2).

Evolutionary rate ratios were calculated and are given in Table 6. Significant ratios were observed between leg development groups with limbless having 2.8 times higher rate to four-legged taxa. Significant ratios were also observed between habitat groups, with a 48 times higher rate between the highest and lowest rates, semi-fossorial and combination semi-aquatic, arboreal, and terrestrial, respectively. Investigating the pairwise ratios of habitat groups, semi-fossorial taxa had significantly higher rates of evolution compared to all other groups (Table 6). No other significant rates were observed between any habitat group combination.

Phylogenetic signal analysis revealed a K-statistic of .0816 (p=.025), indicating a strong bias for shape disparity being attributed to phylogeny (Figure 9).

Biomechanical Analysis

One-way PERMANOVAs were conducted for each set of groupings. Summaries of each test, including Bonferroni-corrected p-values are given in Tables 3-5. For diet, a statistically significant difference was observed for anterior mechanical advantage between carnivores and omnivores. Significant differences were observed for leg development between anterior and opening mechanical advantage. Anterior mechanical advantage differences based in terrestrial and fossorial.

Chapter IV:

Discussion

Main Findings

This study evaluated the relationship between ecological features (diet, leg development, and habitat) with overall jaw shape and biomechanics in Lepidosauria. Geometric morphometrics revealed a link between limb development and jaw shape. It should be noted that phylogeny also plays a role in shape disparity. Interestingly, previous studies have discovered connections between skull shape in squamates and limb development (Yaryhin, Klembara, Pichugin, Kaucka, & Werneburg, 2021). This might indicate that overall head anatomy may have an evolutionary influence on squamate leg development or vise versa.

Rates of evolution were distinct between legless and limbed taxa. This might be explained considering specialized feeding systems present in legless species, namely amphisbaenians and snakes. For example, amphisbaenians have specialized jaw joints that aid in keeping prey fixed when feeding (Gans, 1978). This might, over time, allow for better feeding underground. Specialized, prehensive jaws of snakes that allow for swallowing whole prey may also describe this disparity in evolutionary rate. The disparity in jaw shape between these groups (and among the others) are further emphasized in the principal component data. Semi-fossorial taxa would need to evolve jaw morphology to allow for the optimization of variety of prey which they typically require (R. M. Andrews, Pough, Collazo, & de Queiroz, 1987).

Anterior and opening mechanical advantage are also shown here to have a relationship with leg development. With four-legged taxa having lower anterior mechanical advantage and higher opening mechanical advantage on average compared to limbless taxa, they have weaker, more rapid biters but have slower mouth openings. A significant anterior mechanical advantage difference was observed between carnivores and omnivores, which was consistent with what has been observed in mammals (Morales-García et al., 2021). There were no connections to anterior mechanical advantage and herbivory. However, of note, this study had very low representation of herbivores. Anterior mechanical advantage differences were only observed between fossorial and terrestrial taxa.

There were no connections drawn between dietary preferences and jaw morphology, except for a significant disparity of anterior mechanical advantage in carnivores and omnivores. Again, it should be noted that this study had a low representation of herbivores. Previous studies have noted influences dietary preferences have on skull morphology (Klaczko, Sherratt, & Setz, 2016; Watanabe et al., 2019), so cranial morphology might be the principal indicator for morphological and biomechanical function.

Limitations and Future Directions

The largest limitation of this study was the smaller than anticipated sample size due to limited availability of specimens. This possibly led to the low representation of herbivores in this study. Greater representation amongst all dietary groups could possibly allow for better evaluation of significant differences between herbivores and the other dietary groups. Deliberate selection and inclusion of herbivorous taxa of squamates (or

broader monophyletic reptilian groups) could provide for a more comprehensive evaluation of ecomorphological characteristics.

It may also be helpful to establish a more simplified system for categorizing habitats, especially for multi-substrate taxa. This would possibly allow for fewer but more represented groups for examining habitat relationships to jaw morphology.

With the relationship of jaw morphology and limb development being consistent with skull development and jaw morphology, it might be advantageous to conduct a morphological study using whole-head skeletal landmarking and biomechanical measurements that are both jaw- and cranium-dependent. This would allow for more consideration to be given to muscular attachments in relation to cranial and mandibular orientations. For example, one could use origination and insertion points of the pseudotemporalis and pterygomandibularis relative to the mandibular joint to calculate the moment arm of resistance to evaluate mechanical advantage. This might provide a more comprehensive understanding of head form and ecological function.

Appendix:

Tables and Figures

Table 1: List of species included in this study.

ID	Species	Specimen Number	Source	Mandible	Group [i]	Diet [ii]	Leg Development [ii]	Habitat [ii]
33	Acontias plumbeus	MCZ R-14233	Photo	Right	Scincoidea	Carnivorous	Limbless	Fossorial and Terrestrial
4	Agama agama	FMNH 22190	Photo	Left	Iguania	Omnivorous	Four-legged	Saxicolous and Arboreal
27	Amphisbaena alba	FMNH 195924	Morphosource	Right	Amphisbaenia	Carnivorous	Limbless	Fossorial and Terrestrial
30	Anilius scytale[iii]	USNM 204078	Morphosource	Right	Serpentes	Carnivorous	Limbless	Terrestrial
10	Anniella pulchra	FMNH 130479	Morphosource	Right	Anguiformes	Carnivorous	Limbless	Fossorial
12	Bipes biporus	CAS 126478	Morphosource	Right	Amphisbaenia	Carnivorous	Limbless	Fossorial
48	Broadleysaurus major	MCZ R-141077	Morphosource	Right	Scincoidea	Omnivorous	Four-legged	Terrestrial and Saxicolous
14	Celestus enneagrammus	FMNH 108860	Morphosource	Right	Anguiformes	Carnivorous	Four-legged	Terrestrial
20	Coleonyx variegatus	YPM HERR 014383	Morphosource	Right	Gekkota	Carnivorous	Four-legged	Terrestrial
13	Cordylus namakuiyus	CAS 254912	Morphosource	Right	Scincoidea	Carnivorous	Four-legged	Saxicolous
44	Crotaphytus collaris	FMNH 48667	Morphosource	Right	Iguania	Carnivorous	Four-legged	Terrestrial and Saxicolous
25	Cylindrophis aruensis[iv]	FMNH 60958	Morphosource	Right	Serpentes	Carnivorous	Limbless	Terrestrial
3	Dactylocnemis pacificus	MCZ 141789	photo	Right	Gekkota	Omnivorous	Four-legged	Terrestrial and Arboreal

40	Dibamus novaeguineae	CAS 26937	Morphosource	Right	Dibamidae	Carnivorous	Limbless	Fossorial
18	Elgaria multicarinata	LSUMZ 83406	Morphosource	Right	Anguiformes	Carnivorous	Four-legged	Terrestrial
17	Feylinia currori	MCZ R-42886	Photo	Left	Scincoidea	Carnivorous	Limbless	Fossorial and Terrestrial
6	Gekko gecko	UF 83669	Morphosource	Right	Gekkota	Carnivorous	Four-legged	Arboreal and Saxicolous
22	Heloderma horridum	TNHC 64380	Morphosource	Right	Anguiformes	Carnivorous	Four-legged	Terrestrial
9	Hoplocercus spinosus	UF 69436	Morphosource	Right	Iguania	Carnivorous	Four-legged	Terrestrial
41	Iguana iguana	CM 114410	Photo	Right	Iguania	Herbivorous	Four-legged	Arboreal
36	Lacerta viridis	YPM HERR 012858	Morphosource	Right	Lacertoidea	Omnivorous	Four-legged	Terrestrial and Arboreal
34	Lanthanotus borneensis	FMNH 148589	Morphosource	Right	Anguiformes	Carnivorous	Four-legged	Fossorial
26	Leiocephalus carinatus	AMNH R 57461	photo	Right	Iguania	Omnivorous	Four-legged	Terrestrial and Arboreal
15	Lepidophyma flavimaculatum	LACM 128570	Morphosource	Right	Scincoidea	Carnivorous	Four-legged	Terrestrial
42	Lialis burtonis	FMNH 166958	Digimorph	Left	Gekkota	Carnivorous	Limbless	Terrestrial
45	Lichanura trivirgata[v]	YPM HERR 012869	Morphosource	Right	Serpentes	Carnivorous	Limbless	Terrestrial
35	Liolaemus bellii	MVZ:HERP:125659	Morphosource	Right	Iguania	Omnivorous	Four-legged	Terrestrial and Saxicolous
43	Oplurus cyclurus	YPM HERR 012861	Morphosource	Right	Iguania	Carnivorous	Four-legged	Arboreal
24	Petracola ventrimaculatus	CJB 571	Photo	Right	Lacertoidea	Carnivorous	Four-legged	Terrestrial

39	Plestiodon fasciatus	YPM HERR 012689	Morphosource	Right	Scincoidea	Carnivorous	Four-legged	Terrestrial
2	Polychrus marmoratus	FMNH 42501	Morphosource	Right	Iguania	Omnivorous	Four-legged	Terrestrial and Arboreal
28	Pristidactylus torquatus	FMNH 206964	Morphosource	Right	Iguania	Carnivorous	Four-legged	Arboreal and Saxicolous
37	Pseudopus apodus[vi]	YPM HERR 012870	Morphosource	Right	Anguiformes	Carnivorous	Limbless	Terrestrial
29	Pygopus lepidopodus	CAS 135450	Morphosource	Right	Gekkota	Carnivorous	Limbless	Terrestrial
31	Python molurus [v]	UF 190353	Morphosource	Right	Serpentes	Carnivorous	Limbless	Arboreal
46	Rhineura floridana	FMNH 31774	Morphosource	Right	Amphisbaenia	Carnivorous	Limbless	Fossorial
19	Sceloporus undulatus	NCSM 83600	Morphosource	Right	Iguania	Carnivorous	Four-legged	Terrestrial
32	Sphenodon punctatus[vii]	FMNH 11113	Photo	Right	Sphenodontia	Carnivorous	Four-legged	Terrestrial
23	Stenocercus guentheri	FMNH 27674	Morphosource	Right	Iguania	Carnivorous	Four-legged	Terrestrial and Saxicolous
7	Teius teyou	FMNH 10873	Morphosource	Right	Lacertoidea	Omnivorous	Four-legged	Terrestrial
38	Trioceros jacksonii	AMNH R 84559	Photo	Right	Iguania	Carnivorous	Four-legged	Arboreal
21	Trogonophis wiegmanni	FMNH 109462	Morphosource	Right	Amphisbaenia	Carnivorous	Limbless	Fossorial
1	Tupinambis teguixin	FMNH 22416	Morphosource	Right	Lacertoidea	Omnivorous	Four-legged	Terrestrial
11	Uromastyx aegyptia	FMNH 78661	Morphosource	Right	Iguania	Herbivorous	Four-legged	Terrestrial
47	Varanus salvator	FMNH 35144	Morphosource	Right	Anguiformes	Carnivorous	Four-legged	Semi-aquatic, Arboreal, and Terrrestrial

5	Xantusia vigilis	LACM 123671	Morphosource	Right	Scincoidea	Carnivorous	Four-legged	Saxicolous
16	Xenopeltis unicolor[viii]	FMNH 148900	Morphosource	Right	Serpentes	Carnivorous	Limbless	Semi-Fossorial
8	Xenosaurus grandis	FMNH 123702	Morphosource	Right	Anguiformes	Carnivorous	Four-legged	Saxicolous

[i] From Uetz (2021).
[ii] From Meiri (2018) unless otherwise noted.
[iii] Ecological data from Bittencourt-Silva and Wilkinson (2018).
[iv] Ecological data from Hill (2019).
[v] Ecological data from O'Shea (2007) and "Encyclopedia of Life.")
[vi] Ecological data from Klembara, Yaryhin, Majerová, and Hain (2022) and Hill (2019).
[vii] Ecological data from "Encyclopedia of Life."); "Sphenodon punctatus")
[viii] Ecological data from O'Shea (2007).

Table 2: Summary of Procrustes ANOVAs for jaw shape as a function of diet, leg development, and habitat.

PROCRUSTES ANOVA FOR JAW SHAPE AS A FUNCTION OF DIET							
	Df	SS	MS	Rsq	F	Z	Pr(>F)
Diet	2	0.12819	0.064097	0.06163	1.4778	1.0465	0.144
Residuals	45	1.95186	0.043375	0.93837			
Total	47	2.08005					

PROCRUSTES ANOVA FOR JAW SHAPE AS A FUNCTION OF LEG DEVELOPMENT							
	Df	SS	MS	Rsq	F	Z	Pr(>F)
Leg Development	1	0.11784	0.117843	0.05665	2.7626	1.9307	**0.029**
Residuals	46	1.96221	0.042657	0.94335			
Total	47	2.08005					

PROCRUSTES ANOVA FOR JAW SHAPE AS A FUNCTION OF HABITAT							
	Df	SS	MS	Rsq	F	Z	Pr(>F)
Habitat	10	0.73409	0.073409	0.35292	2.018	2.2234	**0.013**
Residuals	37	1.34597	0.036377	0.64708			
Total	47	2.08005					

Significant p-values ($p<.05$) indicated in bold

Table 3: Pairwise, Bonferroni-corrected p-values of PERMANOVAs of biomechanical markers as a function of diet. Significant p-values (p<.05) indicated in bold.

Total Mandibular Length			Quadrate Articular Offset			Relative Length of Dental Row		
F=.9198	Carnivorous	Omnivorous	F=1.176	Carnivorous	Omnivorous	F=2.495	Carnivorous	Omnivorous
Omnivorous	1		Omnivorous	1		Omnivorous	0.0882	
Herbivorous	0.8667	1	Herbivorous	0.3873	1	Herbivorous	1	0.5787
Anterior Mechanical Advantage			**Posterior Mechanical Advantage**			**Opening Mechanical Advantage**		
F=6.473	Carnivorous	Omnivorous	F=0.06747	Carnivorous	Omnivorous	F=1.116	Carnivorous	Omnivorous
Omnivorous	**0.0024**		Omnivorous	1		Omnivorous	0.5637	
Herbivorous	1	0.2295	Herbivorous	1	1	Herbivorous	1	1

Table 4: Pairwise, Bonferroni-corrected p-values of PERMANOVAs of biomechanical markers as a function of leg development. Significant p-values ($p<.05$) indicated in bold.

Total Mandibular Length		Quadrate Articular Offset		Relative Length of Dental Row	
F=2.15	Limbless	F=0.8381	Limbless	F=1.5	Limbless
Four-legged	0.1051	Four-legged	0.4187	Four-legged	0.2196
Anterior Mechanical Advantage		**Posterior Mechanical Advantage**		**Opening Mechanical Advantage**	
F=8.303	Limbless	F=0.01692	Limbless	F=7.058	Limbless
Four-legged	**0.006**	Four-legged	0.8975	Four-legged	**0.0048**

Table 5: Pairwise, Bonferroni-corrected p-values of PERMANOVAs of anterior mechanical advantage as a function of habitat. Significant p-values ($p<.05$) indicated in bold.

F=5.94	Fossorial and Terrestrial	Saxicolous and Arboreal	Terrestrial	Fossorial	Terrestrial and Saxicolous	Saxicolous	Terrestrial and Arboreal	Arboreal and Saxicolous	Arboreal	Semi-aquatic, Arboreal, and Terrrestrial
Fossorial and Terrestrial										
Saxicolous and Arboreal	1									
Terrestrial	0.4125	1								
Fossorial	1	1	**0.0385**							
Terrestrial and Saxicolous	1	1	1	0.3135						
Saxicolous	1	1	1	1	1					
Terrestrial and Arboreal	1	1	1	0.2475	1	1				
Arboreal and Saxicolous	1	1	1	1	1	1	1			
Arboreal	1	1	1	0.4895	1	1	1	1		
Semi-aquatic, Arboreal, and Terrestrial	1	1	1	1	1	1	1	1	1	
Semi-Fossorial	1	1	1	1	1	1	1	1	1	1

Table 6: Comparative rates of change among groups from compare.evol.rates analysis. Significant p-values (p<.05) indicated in bold. Further pairwise ratios and p-values for categories with significant rate ratios.

	Sigma Rate Ratio	p-value
Group	8.6815	0.256
Diet	2.5143	0.349
Leg Development	2.8186	**0.002**
Habitat	48.4653	**0.007**
Pairwise Rate Ratios and p-values for habitat (Semi-fossorial vs…)		
	Sigma Rate Ratio	p-value
Arboreal	16.0389	**0.01**
Arboreal and Saxicolous	16.5402	**0.013**
Fossorial	11.4191	**0.0215**
Fossorial and Terrestrial	20.8585	**0.011**
Saxicolous	23.2566	**0.005**
Semi-aquatic, Arboreal, and Terrestrial	48.4653	**0.007**
Terrestrial	15.9594	**0.0115**
Terrestrial and Arboreal	30.6793	**0.0025**
Terrestrial and Saxicolous	18.6440	**0.012**

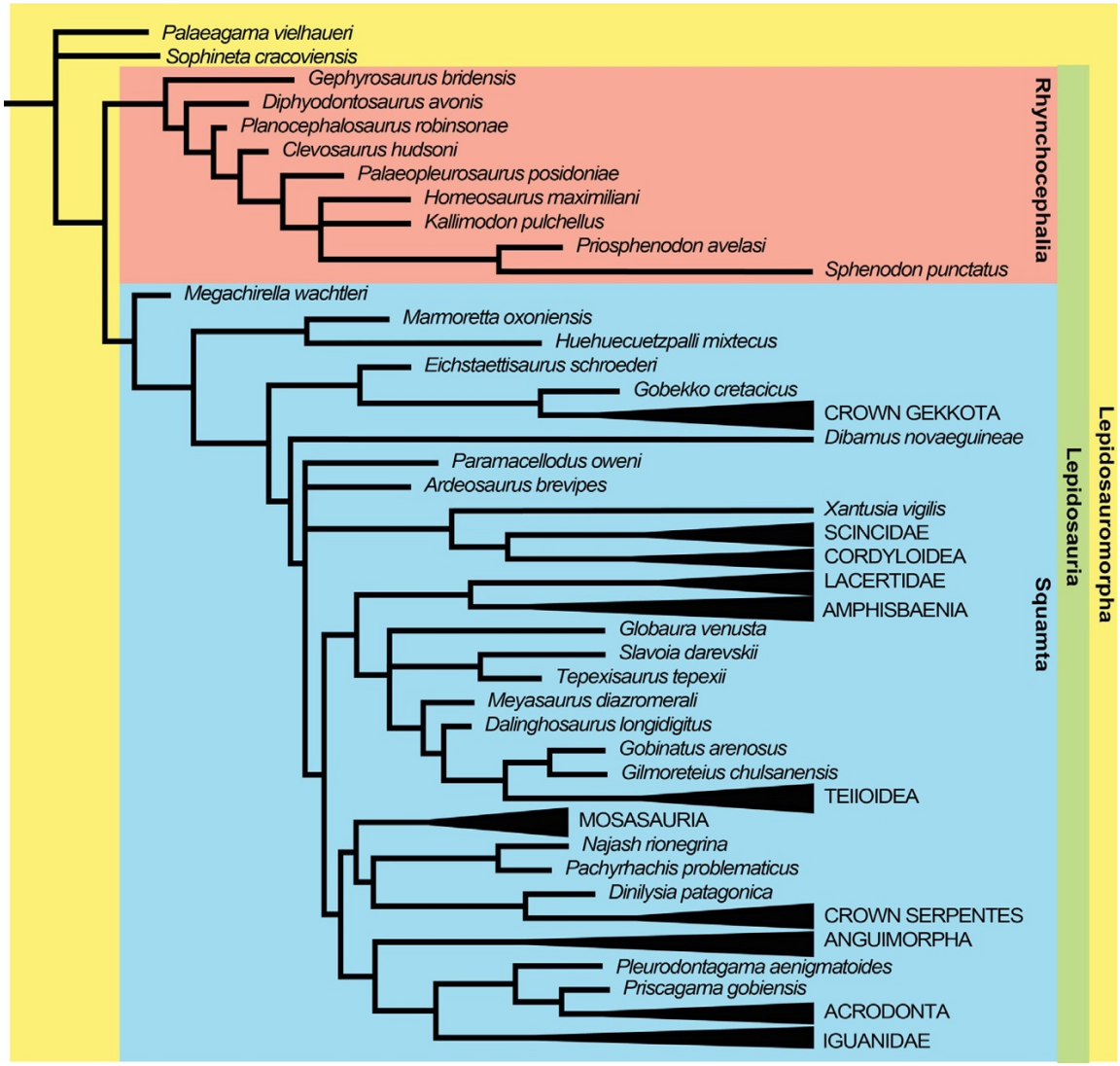

Figure 1. Phylogeny of Lepidosauria. *Phylogeny of Lepidosauria from Simões and Caldwell (2021).*

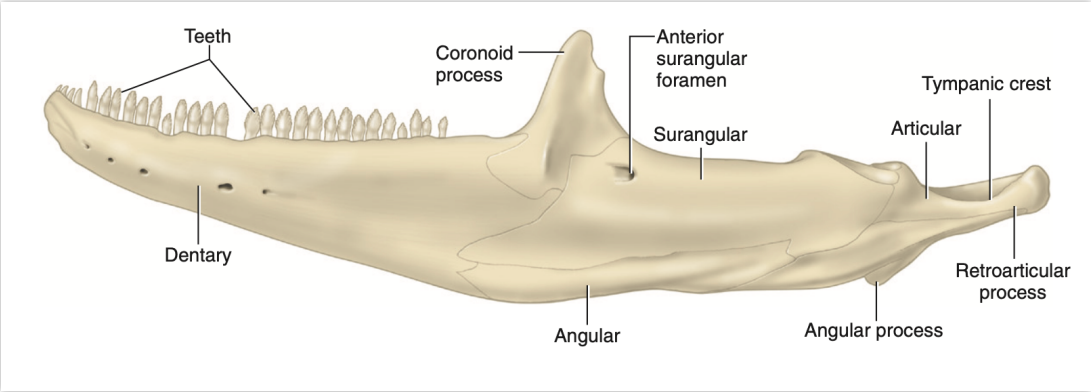

Figure 2. Squamate Jaw Anatomy. *Diagram of the squamate jaw from De Iuliis and Pulerà (2011).*

Landmarks	
LM1	anterior end of anterior tooth
LM2	anterior point of dentary
LM3	anterior point of surangular
LM4	anterior point of angular
LM5	antero-ventral point of dentary-angular suture in lateral view
LM6	postero-ventral point of dentary-angular suture in lateral view
LM7	posterior point of angular
LM8	posterior point of retroarticular process
LM9	dorsal point of retroarticular process
LM10	anterior end of tympanic crest
LM11	dorsal point of coronoid-surangular suture in lateral view
LM12	dorsal point of the coronoid dorsal process
LM13	Posterior end of the coronoid process of the dentary projection of dentary
LM14	posterior end of posterior tooth row
LM15	Posterior end of surangular process of the dentary
LM16	Anterior surangular foramen
LM17	Anterior end of the labial process of the coronoid
Sliding Semi-landmarks	
	20 semi-landmarks appended to curve 1, between LM 2 and 5
	10 semi-landmarks appended to curve 2, between LM 5 and 8
	5 semi-landmarks appended to curve 3, between LM 9 and 10
	15 semi-landmarks appended to curve 4, between LM 10 and 12
	20 semi-landmarks appended to curve 5, between LM 14 and 1

Figure 3. Landmarks and Semi-landmarks. *Diagram of the landmarks and semi-landmarks for geometric morphometric analysis. Stationary landmarks noted in blue. Sliding semi-landmarks noted in red.*

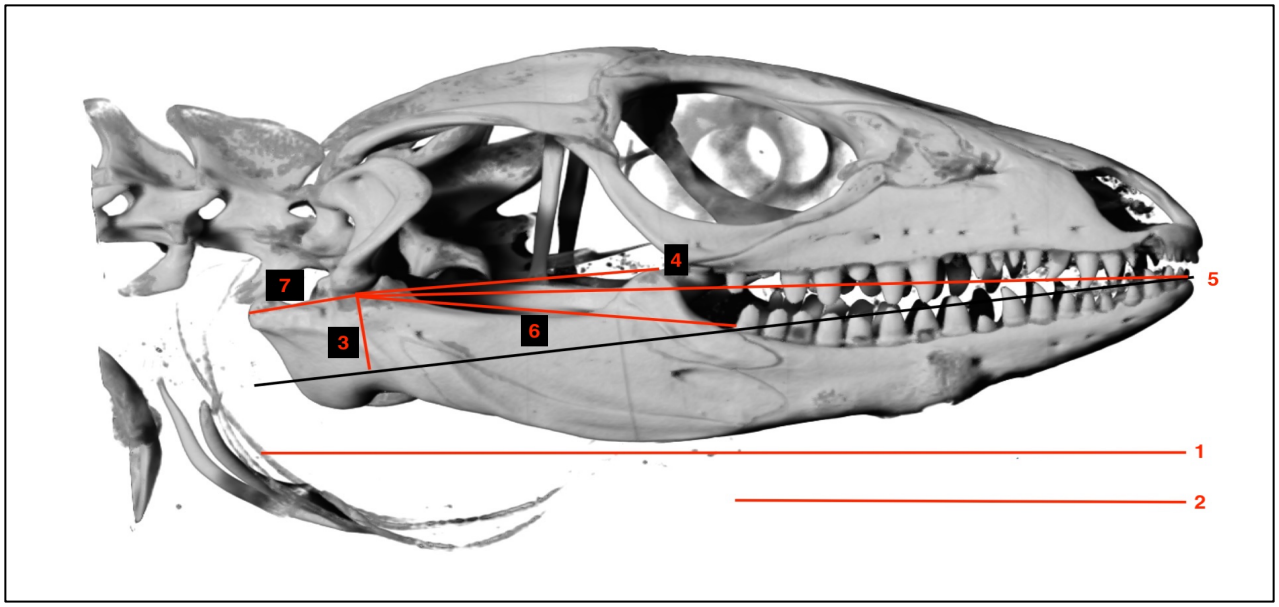

Figure 4. Biomechanical Attributes. *Diagram of the biomechanical measurements investigated in this study. Total mandibular length given by line 1. Relative length of the dental row is the ratio of lines 2 and 1. Quadrate articular offset is given by line 3. Anterior mechanical advantage is given by the ratio of lines 4 and 5. Posterior mechanical advantage is given by the ratio of lines 4 and 6. Opening mechanical advantage is given by the ratio of lines 4 and 7.*

Figure 5. Deformation Grids of Principal Components. *Deformation grids corresponding to extreme principal component scores of principal component analysis of the Procrustes coordinates.*

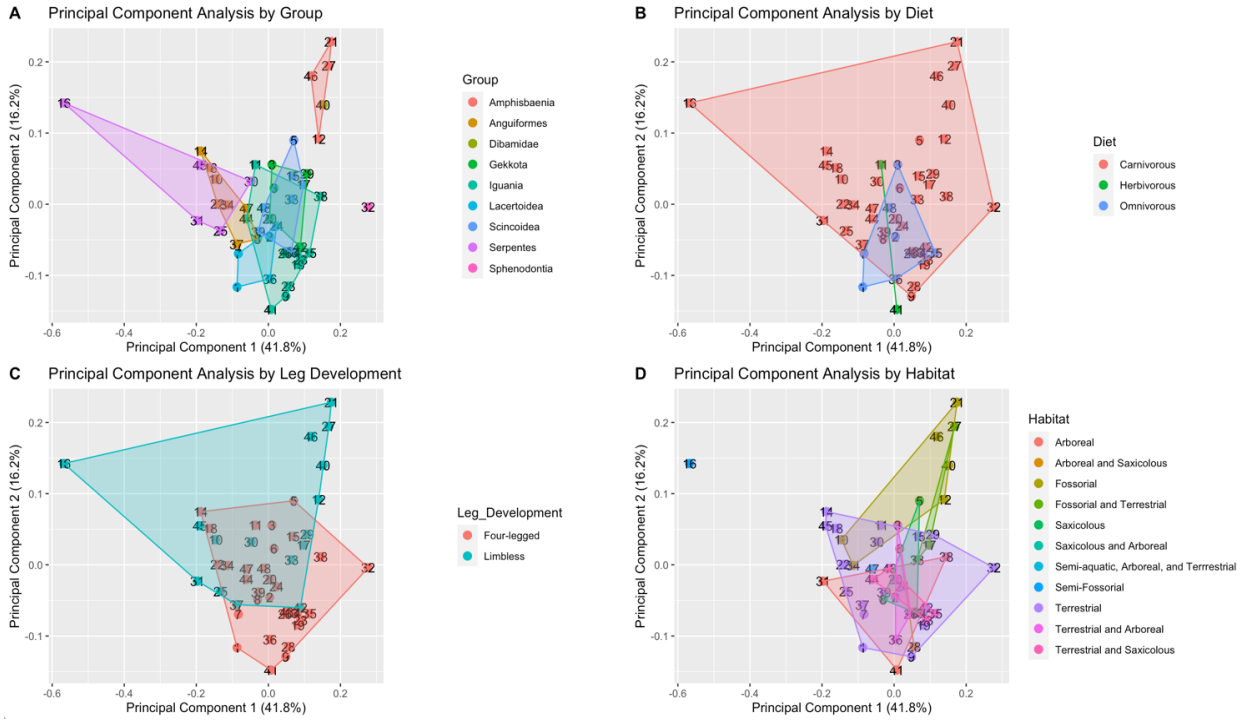

Figure 6. Principal Component Plots. *PCA plots of principal component analysis of Procrustes coordinates. Convex hulls categorize specimens by* ***A.*** *taxonomic group,* ***B.*** *diet,* ***C.*** *leg development, and* ***D.*** *habitat.*

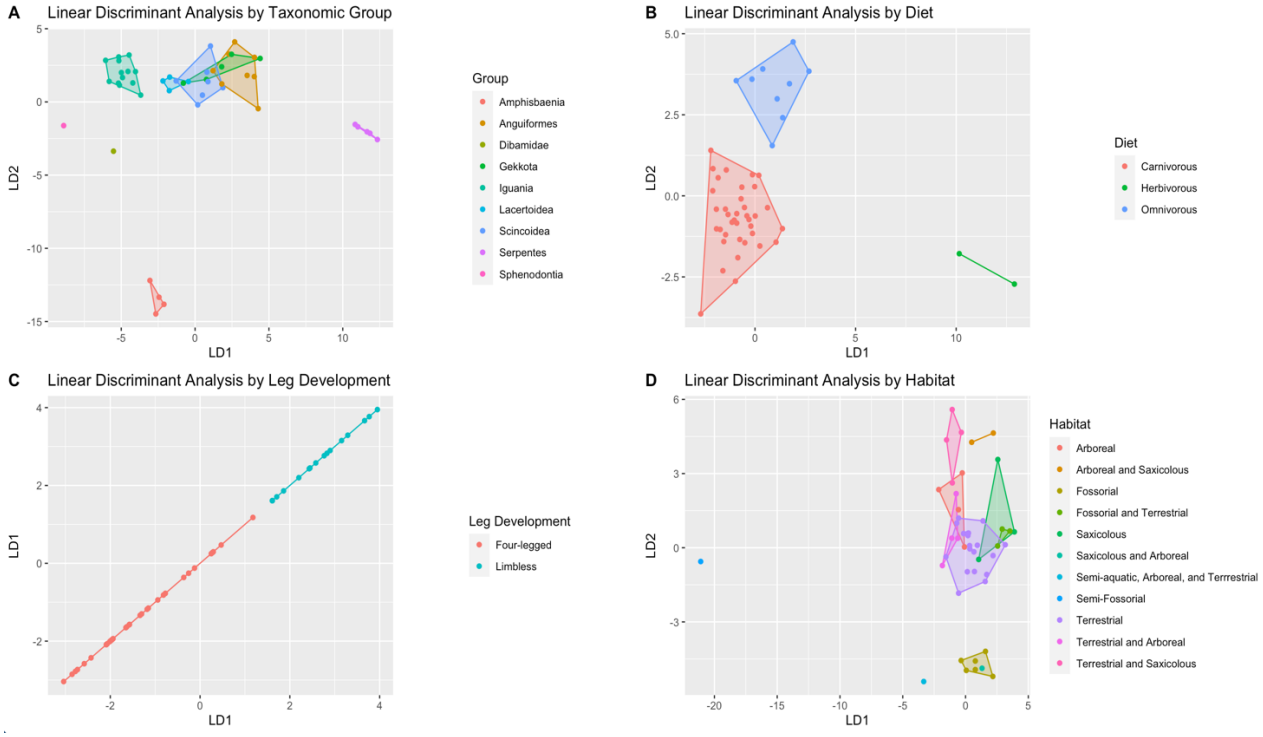

Figure 7. Linear Discriminant Analysis Plots. *LDA plots for linear discriminant analysis by A. taxonomic group, B diet, C. leg development, and D. habitat.*

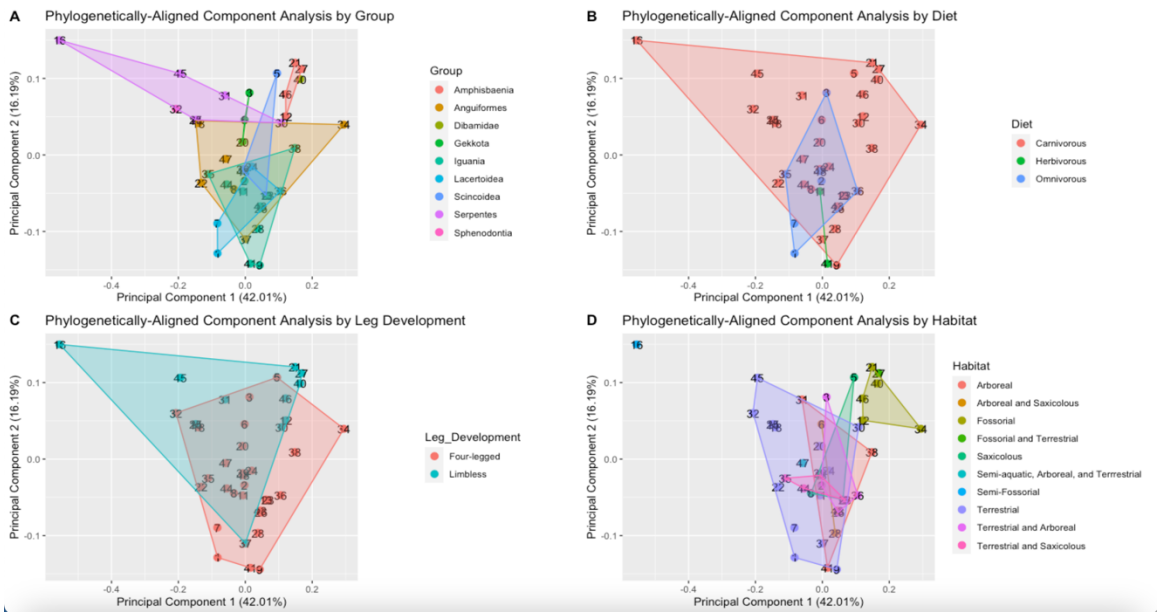

Figure 8. Phylogenetically-Aligned Component Plots. *PaCA plots of phylogenetically-aligned principal component analysis of Procrustes coordinates. Convex hulls categorize specimens by* ***A.*** *taxonomic group,* ***B.*** *diet,* ***C.*** *leg development, and* ***D.*** *habitat.*

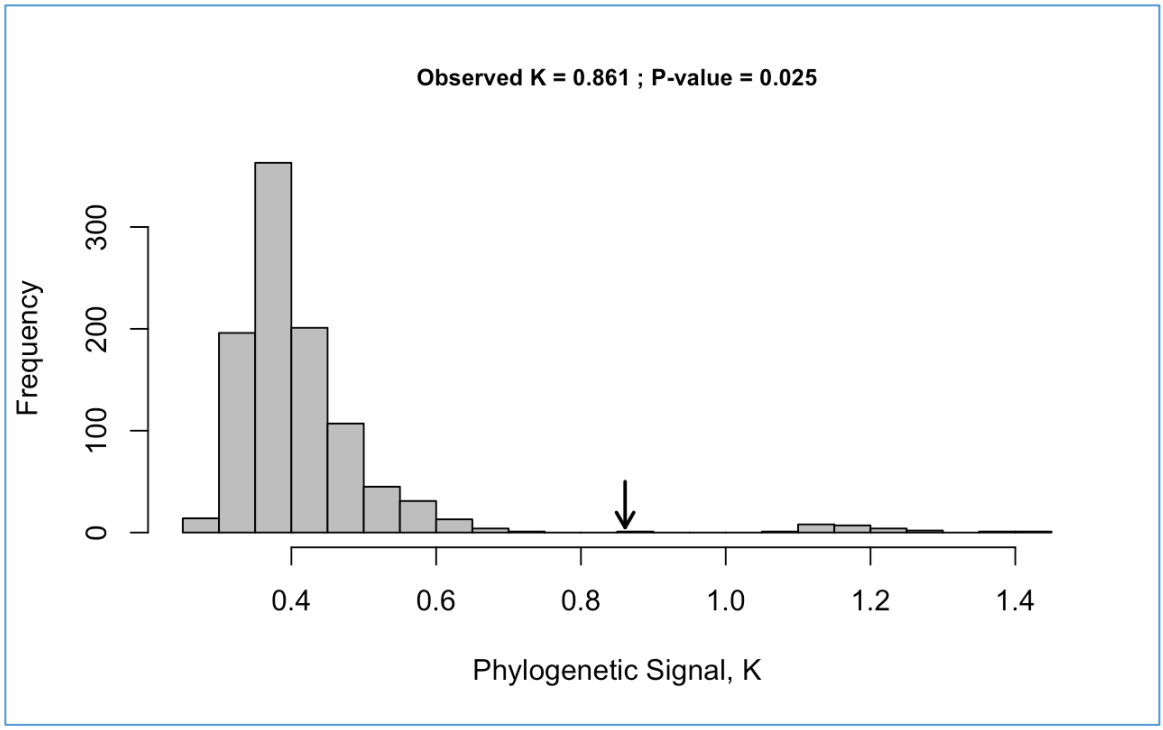

Figure 9. Histogram of K-Statistics from phylogenetic signal analysis.

References

Adams, D. C., M. L. Collyer, A. Kaliontzopoulou, and E.K. Baken. (2022). Geomorph: Software for geometric morphometric analyses. R package version 4.0.4. Retrieved from https://cran.r-project.org/package=geomorph

Alifanov, V. R. (2019). Lizards of the Families Eoxantidae, Ardeosauridae, Globauridae, and Paramacellodidae (Scincomorpha) from the Aptian–Albian of Mongolia. *Paleontological Journal, 53*(1), 74-88. doi:10.1134/S0031030119010039

Anderson, P. S. L. (2009). Biomechanics, functional patterns, and disparity in Late Devonian arthrodires. *Paleobiology, 35*(3), 321-342. doi:10.1666/0094-8373-35.3.321

Anderson, P. S. L., & Westneat, M. W. (2007). Feeding mechanics and bite force modelling of the skull of Dunkleosteus terrelli, an ancient apex predator. *Biology letters (2005), 3*(1), 77-80. doi:10.1098/rsbl.2006.0569

Andrews, R. (2015). The Biology of Chameleons. In: The University of Chicago Press.

Andrews, R. M., Pough, F. H., Collazo, A., & de Queiroz, A. (1987). The ecological cost of morphological specialization: feeding by a fossorial lizard. *Oecologia, 73*(1), 139-145. doi:10.1007/BF00376990

Baken, E. K., M. L. Collyer, A. Kaliontzopoulou, and D. C. Adams. (2021). geomorph v4.0 and gmShiny: enhanced analytics and a new graphical interface for a comprehensive morphometric experience.: Methods in Ecology and Evolution.

Bittencourt, J. S., Simoes, T. R., Caldwell, M. W., & Langer, M. C. (2020). Discovery of the oldest South American fossil lizard illustrates the cosmopolitanism of early South American squamates. *Communications biology, 3*(1), 201-201. doi:10.1038/s42003-020-0926-0

Bittencourt-Silva, G. B., & Wilkinson, M. (2018). First record of predation on the caecilian Microcaecilia unicolor (Duméril, 1863). *Herpetology Notes, 11*, 641-644.

Bourke, J., Wroe, S., Moreno, K., McHenry, C., & Clausen, P. (2008). Effects of Gape and Tooth Position on Bite Force and Skull Stress in the Dingo (Canis lupus dingo) Using a 3-Dimensional Finite Element Approach. *PloS one, 3*(5), e2200-e2200. doi:10.1371/journal.pone.0002200

Conrad, J. L., Ast, J. C., Montanari, S., & Norell, M. A. (2011). A combined evidence phylogenetic analysis of Anguimorpha (Reptilia: Squamata). *Cladistics, 27*(3), 230-277. doi:10.1111/j.1096-0031.2010.00330.x

Da Silva, F. O., Fabre, A.-C., Savriama, Y., Ollonen, J., Mahlow, K., Herrel, A., . . . Di-Poï, N. (2018). The ecological origins of snakes as revealed by skull evolution. *Nature Communications, 9*(1), 376.

De Iuliis, G., & Pulerà, D. (2011). CHAPTER 8 - Reptile Skulls and Mandibles. In (Second Edition ed., pp. 253-285): Elsevier Inc.

Encyclopedia of Life. Retrieved from http://eol.org

Evans, S. E., & Jones, M. E. H. (2010). The Origin, Early History and Diversification of Lepidosauromorph Reptiles. In *New Aspects of Mesozoic Biodiversity* (pp. 27-44). Berlin, Heidelberg: Springer Berlin Heidelberg.

Gamble, T., Greenbaum, E., Jackman, T. R., Russell, A. P., & Bauer, A. M. (2017). Repeated evolution of digital adhesion in geckos: a reply to Harrington and Reeder. *Journal of Evolutionary Biology, 30*(7), 1429-1436. doi:https://doi.org/10.1111/jeb.13097

Gans, C. (1978). The characteristics and affinities of the Amphisbaenia. *The Transactions of the Zoological Society of London, 34*(4), 347-416.

Gill, P. G., Purnell, M. A., Crumpton, N., Brown, K. R., Gostling, N. J., Stampanoni, M., & Rayfield, E. J. (2014). Dietary specializations and diversity in feeding ecology of the earliest stem mammals. *Nature (London), 512*(7514), 303-305. doi:10.1038/nature13622

Greer, A. E. (1985). The Relationships of the Lizard Genera Anelytropsis and Dibamus. *Journal of Herpetology, 19*(1), 116-156. doi:10.2307/1564427

Haas, G. (1973). Muscles of the jaws and associated structures in the Rhynchocephalia and Squamata. *Biology of the Reptilia, 4*(5), 285-490.

Hammer, Ø., Harper, D. A., & Ryan, P. D. (2001). PAST: Paleontological statistics software package for education and data analysis. *Palaeontologia electronica, 4*(1), 9.

Herrera-Flores, J. A., Stubbs, T. L., Benton, M. J., & Ruta, M. (2017). Macroevolutionary patterns in Rhynchocephalia: is the tuatara (Sphenodon punctatus) a living fossil? *Palaeontology, 60*(3), 319-328. doi:10.1111/pala.12284

Hill, R. L. (2019). Squamata Diet. In J. Vonk & T. Shackelford (Eds.), *Encyclopedia of Animal Cognition and Behavior* (pp. 1-13). Cham: Springer International Publishing.

Hsiang, A. Y., Field, D. J., Webster, T. H., Behlke, A. D. B., Davis, M. B., Racicot, R. A., & Gauthier, J. A. (2015). The origin of snakes: revealing the ecology, behavior, and evolutionary history of early snakes using genomics, phenomics,

and the fossil record. *BMC Evolutionary Biology, 15*(1), 87. doi:10.1186/s12862-015-0358-5

Jones, M. E. H., Curtis, N., O'Higgins, P., Fagan, M., & Evans, S. E. (2009). The head and neck muscles associated with feeding in Sphenodon (Reptilia, Lepidosauria, Rhynchocephalia). *Palaeontologia electronica, 12*(2).

Klaczko, J., Sherratt, E., & Setz, E. Z. (2016). Are diet preferences associated to skulls shape diversification in xenodontine snakes? *PloS one, 11*(2), e0148375.

Klembara, J., Yaryhin, O., Majerová, J., & Hain, M. (2022). Comparative anatomy and ontogeny of appendicular skeleton of Pseudopus apodus (Pallas, 1775) (Anguimorpha, Anguidae) and a pattern of hindlimb loss in Anguinae. *Anatomical record (Hoboken, N.J. : 2007), 305*(9), 2290-2311. doi:10.1002/ar.24851

Lind, A. L., Lai, Y. Y. Y., Mostovoy, Y., Holloway, A. K., Iannucci, A., Mak, A. C. Y., . . . Bruneau, B. G. (2019). Genome of the Komodo dragon reveals adaptations in the cardiovascular and chemosensory systems of monitor lizards. *Nature Ecology & Evolution, 3*(8), 1241-1252. doi:10.1038/s41559-019-0945-8

McDowell, S. B. (1986). The Architecture of the Corner of the Mouth of Colubroid Snakes. *Journal of Herpetology, 20*(3), 353-407. doi:10.2307/1564502

Meiri, S. (2018). Traits of lizards of the world: Variation around a successful evolutionary design. *Global ecology and biogeography, 27*(10), 1168-1172. doi:10.1111/geb.12773

Mizuno, T., & Kojima, Y. (2015). A blindsnake that decapitates its termite prey. *Journal of Zoology, 297*(3), 220-224. doi:https://doi.org/10.1111/jzo.12268

Morales-García, N. M., Gill, P. G., Janis, C. M., & Rayfield, E. J. (2021). Jaw shape and mechanical advantage are indicative of diet in Mesozoic mammals. *Communications biology, 4*(1), 242. doi:10.1038/s42003-021-01757-3

O'Shea, M. (2007). *Boas and Pythons of the World*: Princeton University Press.

Oelrich, T. M. (1956). *The anatomy of the head of Ctenosaura pectinata (Iguanidae)*. Ann Arbor: Museum of Zoology, University of Michigan.

ORS. (2020). Dragonfly 2020.2. Montreal, Canada: Object Research Systems. Retrieved from http://www.theobjects.com/dragonfly

Polcyn, M. J., Jacobs, L. L., Araújo, R., Schulp, A. S., & Mateus, O. (2014). Physical drivers of mosasaur evolution. *Palaeogeography, Palaeoclimatology, Palaeoecology, 400*, 17-27. doi:https://doi.org/10.1016/j.palaeo.2013.05.018

Ramsay, J. B., & Wilga, C. D. (2007). Morphology and mechanics of the teeth and jaws of white-spotted bamboo sharks (Chiloscyllium plagiosum). *Journal of morphology (1931), 268*(8), 664-682. doi:10.1002/jmor.10530

Rieppel, O. (1979). A cladistic classification of primitive snakes based on skull structure. *Journal of Zoological Systematics and Evolutionary Research, 17*(2), 140-150. doi:https://doi.org/10.1111/j.1439-0469.1979.tb00696.x

Rohlf, F. J. (2017). tpsDig2, Digitize Landmarks and Outlines, Version 2.31. Stony Brook, NY: Department of Ecology and Evolution, State University of New York.

Schneider, C. A., Rasband, W. S., & Eliceiri, K. W. (2012). NIH Image to ImageJ: 25 years of image analysis. *Nature Methods, 9*(7), 671-675. doi:10.1038/nmeth.2089

Schwenk, K. (2000). CHAPTER 8 - Feeding in Lepidosaurs. In K. Schwenk (Ed.), *Feeding* (pp. 175-291). San Diego: Academic Press.

Simões, T. R., & Caldwell, M. W. (2021). Lepidosauromorphs. In D. Alderton & S. A. Elias (Eds.), *Encyclopedia of Geology (Second Edition)* (pp. 165-174). Oxford: Academic Press.

Simões, T. R., & Pyron, R. A. (2021). THE SQUAMATE TREE OF LIFE. *Bulletin of the Museum of Comparative Zoology, 163*(2), 47-95, 49. Retrieved from https://doi.org/10.3099/0027-4100-163.2.47

Sphenodon punctatus. Retrieved from https://www.reptiles.org.nz/herpetofauna/native/sphenodon-punctatus

Stubbs, T. L., Pierce, S. E., Rayfield, E. J., & Anderson, P. S. L. (2013). Morphological and biomechanical disparity of crocodile-line archosaurs following the end-Triassic extinction. *Proceedings of the Royal Society. B, Biological sciences, 280*(1770), 20131940-20131940. doi:10.1098/rspb.2013.1940

Uetz, P., Freed, P, Aguilar, R. & Hošek, J. (eds.). (2021). The Reptile Database. Retrieved from http://www.reptile-database.org

Venables, W. N. R., B. D. (2002). *Modern Applied Statistics with S* (Fourth ed.): Springer.

Wainwright, P. C., & Richard, B. A. (1995). PREDICTING PATTERNS OF PREY USE FROM MORPHOLOGY OF FISHES. *Environmental biology of fishes, 44*(1-3), 97-113. doi:10.1007/BF00005909

Watanabe, A., Fabre, A.-C., Felice, R. N., Maisano, J. A., Müller, J., Herrel, A., & Goswami, A. (2019). Ecomorphological diversification in squamates from conserved pattern of cranial integration. *Proceedings of the National Academy of Sciences, 116*(29), 14688-14697.

Webster, M., & Sheets, H. D. (2010). A Practical Introduction to Landmark-Based Geometric Morphometrics. *The Paleontological Society Papers, 16*, 163-188. doi:10.1017/S1089332600001868

Westneat, M. W. (2003). A biomechanical model for analysis of muscle force, power output and lower jaw motion in fishes. *Journal of theoretical biology, 223*(3), 269-281. doi:10.1016/S0022-5193(03)00058-4

Yaryhin, O., Klembara, J., Pichugin, Y., Kaucka, M., & Werneburg, I. (2021). Limb reduction in squamate reptiles correlates with the reduction of the chondrocranium: a case study on serpentiform anguids. *Developmental Dynamics, 250*(9), 1300-1317.

Zelditch, M. L., Swiderski, D. L., & Sheets, H. D. (2012). *Geometric Morphometrics for Biologists: A Primer*. San Diego: Elsevier Science & Technology.